

---

# COGNEN: CONSTRUCTING THE KERNEL OF A HYPERDIMENSIONAL PREDICTIVE PROCESSING COGNITIVE ARCHITECTURE

---

**Alexander Ororbia<sup>†</sup>**  
ago@cs.rit.edu

**M. Alex Kelly<sup>‡</sup>**  
alex.kelly@carleton.ca

<sup>†</sup> Rochester Institute of Technology, Rochester, NY, 14623, USA.

<sup>‡</sup> Carleton University, Ottawa, ON, K1S 5B6, Canada.

## ABSTRACT

We present a new cognitive architecture that combines two neurobiologically plausible, computational models: (1) a variant of predictive processing known as neural generative coding (NGC) and (2) hyperdimensional / vector-symbolic models of human memory. We draw inspiration from well-known cognitive architectures such as ACT-R, Soar, Leabra, and Spaun/Nengo. Our cognitive architecture, the COGnitive Neural GENERative system (CogNGen), is in broad agreement with these architectures, but provides a level of detail between ACT-R’s high-level, symbolic description of human cognition and Spaun’s low-level neurobiological description. CogNGen creates the groundwork for developing agents that learn continually from diverse tasks and model human performance at larger scales than what is possible with existent cognitive architectures. We aim to develop a cognitive architecture that has the power of modern machine learning techniques while retaining long-term memory, single-trial learning, transfer-learning, planning, and other capacities associated with high-level cognition. We test CogNGen on a set of maze-learning tasks, including mazes that test short-term memory and planning, and find that the addition of vector-symbolic models of memory improves the ability of the NGC reinforcement learning model to master the maze task. Future work includes testing CogNGen on more tasks and exploring methods for efficiently scaling hyperdimensional memory models to lifetime learning.

**Keywords** Cognitive Architectures · Predictive Processing · Memory · Reinforcement Learning · Active Inference · Neural Generative Coding · Vector-Symbolic Architectures · MINERVA

## 1 Introduction

Modern machine learning techniques based on artificial neural networks (ANNs) are implemented through algebraic manipulations of vectors, matrices, and tensors in high-dimensional spaces. While ANNs have an impressive ability to process data to find patterns, they do not typically model high-level cognition. Furthermore, ANNs are usually models of only a single task. Otherwise, when an ANN is trained to learn a series of tasks, catastrophic interference occurs, with each new task causing the ANN to forget all previously learned tasks [9, 34, 35]. On the other hand, symbolic cognitive architectures, such as the widely used ACT-R [2, 43], can capture the complexities of high-level cognition but scale poorly to the naturalistic, non-symbolic data of sensory perception (e.g., images) or to big data sets necessary for modelling learning over a lifetime (e.g., corpora with hundreds of millions of words).

Are symbolic and ANN approaches compatible? Symbolic and neural models can be understood as theories of cognition operating at different levels of description [26]. Is it possible to provide a theory that bridges these two levels, a reduction of the symbolic to the neural, while retaining the strengths and capabilities of each?

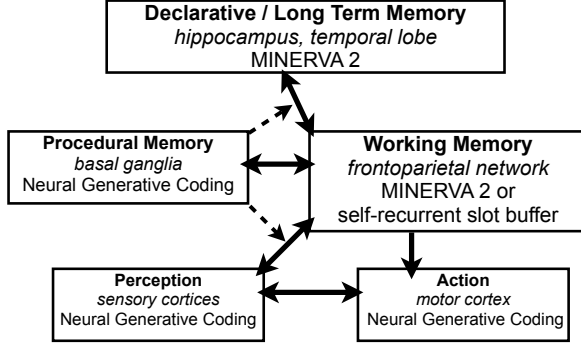


Figure 1: Common Model of Cognition [33], associated brain areas [49, 47, 48] and our approach to modelling each module. Solid arrows are data passing. Dashed arrows are modulation of data passing.

We propose a cognitive architecture that is built on two neurobiologically and cognitively plausible models, namely a variant of predictive processing known as neural generative coding (NGC) [40] and vector-symbolic (a.k.a. hyperdimensional) models of memory [16, 19, 25]. Desirably, the use of these particular building blocks yields naturally scalable, local update rules, based on variants of Hebbian learning [13], to adjust the overall system’s synaptic weight parameters while facilitating robustness in acquiring, storing, and composing distributed representations of tasks encountered sequentially. Our intent is to advance towards a cognitive architecture capable of modeling human performance at all scales of learning, from the half-hour lab experiment to skills acquired gradually over a lifetime. By combining predictive processing with vector-symbolic models of human memory, we work towards creating a model of cognition that has the power of modern machine learning techniques while retaining long-term memory, single-trial learning, transfer-learning, planning, and other cognitive capacities associated with high-level cognition.

While our ultimate aims are lofty, in this paper we demonstrate proof of concept. We show that our architecture, CogNGen (the COGnitive Neural GENerative system), is able to learn variants of a maze-learning task, including mazes that require planning (getting a key to open a locked door) and short-term memory (picking the correct path based on an earlier cue). In the context of reinforcement learning, our results further demonstrate that the synergy between predictive processing circuits and vector-symbolic models of short and long-term memory is competitive with several powerful intrinsic curiosity approaches, offering promising performance when the problem-specific reward is sparse.

## 2 The Common Model of Cognition

Since Newell [37] first argued that good empirical work and piecemeal theoretical work are insufficient to understand the mind, researchers in cognitive science have sought to develop functional, testable theories of cognition as a whole. Cognitive architectures serve as both unified theories of cognition and as computational frameworks for implementing models of specific experimental tasks. Forty years of research has developed hundreds of cognitive architectures, many with strong similarities to each other [28], suggesting an emerging consensus on the basic principles of cognition. The *Common Model of Cognition* [33] is a high-level theory of the modules of the mind and how they interact (see Fig. 1), proposed on the basis of commonalities between three cognitive architectures: ACT-R [1], Soar [32], and SIGMA [44].

The Common Model of Cognition consists of perceptual and motor modules that interact with the agent’s environment, short-term or working memory buffers which hold the active data in the agent’s mind, a declarative or long-term memory module that holds the agent’s world knowledge, and a procedural memory module that controls the flow of information and evaluates possible actions [33]. An evaluation of fMRI data from 200 participants across diverse tasks found correlations in patterns of activity across brain areas consistent with the Common Model of Cognition’s modules and their interactions [49].

## 3 Neural Building Blocks

We start by first formally describing the fundamental neural circuits (building blocks) that are used to construct the various modules of the CogNGen kernel instantiation of the Common Model of Cognition.

### 3.1 Notation

In this work,  $|\mathbf{v}|$  is the cardinality or dimensionality  $D$  of vector  $\mathbf{v} = [v_1, v_2, \dots, v_D]^T$  which we treat as a column vector  $\mathbf{v} \in \mathcal{R}^{D \times 1}$  (or matrix with one column).  $\mathbf{v}_{j,1}$  is the  $j$ th element of the column vector  $\mathbf{v}$  (bold indicates a matrix or vector) represented as a  $1 \times 1$  matrix, whereas  $v_{j,1}$  is the same element represented as a scalar (a distinction of software implementation rather than mathematics). Likewise,  $\mathbf{W}_{i,j}$  and  $W_{i,j}$  are the element at  $i$ th row and  $j$ th column of matrix  $\mathbf{W}$  represented as a  $1 \times 1$  matrix and a scalar respectively.

In terms of operations,  $\leftarrow$  indicates assignment,  $\odot$  indicates a Hadamard product,  $\oslash$  indicates element-wise division, and  $\cdot$  indicates a matrix/vector multiplication (or dot product if operators are vectors of the same shape) and  $\mathbf{v}^T$  denotes the transpose.  $[\mathbf{v}^1, \mathbf{v}^2, \dots, \mathbf{v}^V]$  denotes concatenation of a series of  $V$  vectors  $\mathbf{v}^1, \mathbf{v}^2, \dots, \mathbf{v}^V$  along the row axis (note that it is possible that  $|\mathbf{v}^1| \neq |\mathbf{v}^2| \neq \dots \neq |\mathbf{v}^3|$ , since all that is required is that each vector is a column vector).  $\lfloor \mathbf{v} \rfloor$  is the element-wise floor function applied to vector  $\mathbf{v}$ .

### 3.2 Neural Generative Coding (NGC)

Neural generative coding (NGC) is an instantiation of the predictive processing brain theory [42, 10, 6], yielding an efficient, robust form of predict-then-correct learning and inference.

Specifically, an NGC circuit in our system receives two sensory vectors, an input  $\mathbf{x}^i \in \mathcal{R}^{I \times 1}$  ( $I$  is the input dimensionality) and an output  $\mathbf{x}^o \in \mathcal{R}^{O \times 1}$  ( $O$  is the output or target dimensionality). Compactly, an NGC circuit is composed of  $L$  layers of feedforward neuronal units, i.e., layer  $\ell$  is represented by the state vector  $\mathbf{z}^\ell \in \mathcal{R}^{H_\ell \times 1}$  containing  $H_\ell$  total units. Given the input–output pair of sensory vectors  $\mathbf{x}^i$  and  $\mathbf{x}^o$ , the circuit clamps the last layer  $\mathbf{z}^L$  to the input,  $\mathbf{z}^L = \mathbf{x}^i$ , and clamps the first layer  $\mathbf{z}^0$  to the output,  $\mathbf{z}^0 = \mathbf{x}^o$ . Once clamped, the NGC circuit will undergo a settling cycle where it processes the input and output vectors for  $K$  steps in times, i.e., it process sensory signals over a stimulus window of  $K$  discrete time steps. The activities of the internal neurons (all neurons in between the clamped layers  $\ell = L \dots 0$ ) are updated according to the following equation (formulated for layer  $\ell$ ), as follows:

$$\mathbf{z}^\ell \leftarrow \mathbf{z}^\ell + \beta \left( -\gamma \mathbf{z}^\ell + (-\mathbf{e}^\ell + \mathbf{E}^\ell \cdot \mathbf{e}^{\ell-1}) + \Phi(\mathbf{z}^\ell) \right) \quad (1)$$

where  $\mathbf{E}^\ell$  is the learnable matrix containing error synaptic weights that are meant to pass along mismatch signals from layer  $\ell - 1$  to  $\ell$ .  $\beta$  is the neural state update coefficient (typically set according to  $\beta = \frac{1}{\tau}$ , where  $\tau$  is the integration time constant in the order of milliseconds) and  $\Phi(\cdot)$  is a special lateral interaction function, which we do not use in this paper, i.e.,  $\Phi(\mathbf{v}) = 0$ . This update equation indicates that a vector of neural activity changes, at each step within a settling cycle, according to (from left to right), a leak term/variable (the strength of which is controlled by  $\gamma$ ), a combined top-down and bottom-up pressure from mismatch signals in nearby neural regions/layers, and an optional lateral interaction term.  $\mathbf{e}^\ell \in \mathcal{R}^{H_\ell \times 1}$  are an additional set/population of special neurons that are tasked entirely with calculating mismatch signals at a layer  $\ell$ , i.e.,  $\mathbf{e}^\ell = \mathbf{z}^\ell - \bar{\mathbf{z}}^\ell$ , the difference between a layer's current activity (or clamped value) and an expectation/prediction produced from another layer. Specifically, the layer-wise prediction  $\bar{\mathbf{z}}^\ell$  is computed as follows:  $\bar{\mathbf{z}}^\ell = g^\ell(\mathbf{W}^{\ell+1} \cdot \phi^{\ell+1}(\mathbf{z}^{\ell+1}))$  (with  $\mathbf{W}^\ell$  denoting the learnable matrix of generative/predictive synapses).  $\phi^{\ell+1}$  is the activation function (the linear rectifier in this work) for state variables and  $g^\ell$  is a nonlinearity applied to predictive outputs (the identity in this study).

After processing the input–output pair for  $K$  steps (repeatedly applying Equation 1  $K$  times), the synaptic weight matrices may be adjusted with a Hebbian-like update rule as follows:

$$\Delta \mathbf{W} = \mathbf{e}^\ell \cdot (\phi^{\ell+1}(\mathbf{z}^{\ell+1}))^T \odot \mathbf{M}_W \quad (2)$$

$$\Delta \mathbf{E} = \gamma_e (\Delta \mathbf{W})^T \odot \mathbf{M}_E \quad (3)$$

where  $\gamma_e$  is a factor (less than one) to control the time-scale that the error synapses are evolved (to ensure they change a bit more slowly than the generative synapses).  $\mathbf{M}_W$  and  $\mathbf{M}_E$  are modulation matrices that perform a form a synaptic scaling that ultimately ensures additional stability in the learning process (see [38] for details). All NGC circuits in this work are implemented according to the process mechanistically described above.

Another important functionality of an NGC circuit is the ability to ancestrally project a vector (akin to a feedforward pass, since no settling process is required) through the underlying directed generative model – we will represent this as  $f_{proj}(\mathbf{x}^i; \Theta)$ . Formally, ancestrally projecting a vector  $\mathbf{x}^i$  through an NGC circuit proceeds as follows:

$$\mathbf{z}^\ell = \bar{\mathbf{z}}^\ell = g^\ell(\mathbf{W}^{\ell+1} \cdot \phi^{\ell+1}(\mathbf{z}^{\ell+1})), \forall \ell = (L-1), \dots, 0 \quad (4)$$

where  $\mathbf{z}^L = \mathbf{x}^i$  (the input/top-most layer is clamped to a specific vector, such as current input  $\mathbf{x}^i$ ).

### 3.3 Memory

We simulate both declarative (long-term) and working (short-term) memory using the MINERVA 2 model of human memory [15]. We choose MINERVA 2 since it captures a wide variety of human memory phenomena across differing settings and, as such, seems a good candidate for integration into a cognitive architecture. MINERVA 2 has been applied to a variety of experimental paradigms, including judgement of frequency and recognition [15], category learning [16], implicit learning [18, 19], associative and reinforcement learning phenomena from both the animal and human learning literature [7, 17], heuristics and biases in decision-making [8], hypothesis-generation [50], learning the meaning of words [20, 31], and the production of grammatical sentences [22, 24].

#### 3.3.1 Adding to Memory

MINERVA 2 stores memory traces: observations or sequence of observations of the state of the word. Each memory trace is represented as an array of real numbers (i.e., a vector). MINERVA 2 stores all memory traces separately as rows in a continuously growing table.

The continuous growth of the memory table results in a scaling problem for CogNGen, with significant slow downs even in the small maze learning tasks under consideration in this paper. Most MINERVA 2 models store only a small number of memory traces, though a few MINERVA 2 models used for language processing have stored up to 20,000 [20] to 500,000 traces [21, 24]. With a persistent long-term memory store across learning the maze task, in the worst case, as many as millions of traces might be stored in CogNGen’s memory.

We use MINERVA 2’s forgetting mechanism [16] and randomly delete values from memory each time memory is updated at a sufficiently high probability to impose a computationally tractable limit on the size of MINERVA 2’s memory. Other possible solutions to the unbounded growth of memory are to use a compressed, scale-invariant approximation to MINERVA 2 [25] or to adopt a different memory system that grows only with the number of unique stimuli, rather than with each new sequence of observations [23]. However, exploring these alternative methods for improving the ability of CogNGen’s memory to scale to larger problems is a matter for future work.

#### 3.3.2 Retrieval from Memory

In MINERVA 2, memory retrieval is not a look-up process, it is a reconstruction process. When a retrieval cue is presented, each vector in the memory table is activated in proportion to its similarity to the cue [16]. Similarity is computed as a normalized dot-product of the cue’s vector with the stored vector. Each stored vector is activated by its cubed similarity to the cue. Information is retrieved from memory in the form of a new vector, a weighted sum of the vectors in the table, each vector weighted by its activation:

$$\mathbf{e} = \sum_{i=1}^m \left( \frac{\mathbf{p} \cdot \mathbf{t}_i}{\sqrt{\mathbf{p} \cdot \mathbf{p}} \sqrt{\mathbf{t}_i \cdot \mathbf{t}_i}} \right)^3 \quad (5)$$

where  $\mathbf{e}$  is the retrieved vector,  $\mathbf{t}_i$  is the  $i$ -th trace in memory,  $\mathbf{p}$  is the retrieval cue, and  $m$  is the number of traces in the memory table. By computing activation as the cube of similarity, the contribution of the most similar vectors is emphasized and that of the least similar (and least relevant) is minimized.

Due to its retrieval equation, MINERVA 2 is mathematically equivalent to a type of very large Hebbian associative memory with a fixed number of neurons and a limited storage capacity [25]. However, the Hebbian network is sufficiently large that it is more efficient to simulate the network’s behaviour as a growing table of memory traces. However, MINERVA 2 can be noisily approximated using smaller, more tractable Hebbian associative memory models [25], an alternative we plan to explore in future versions of CogNGen.

#### 3.3.3 Discrepancy Encoding

In CogNGen, we combine insights from several versions of MINERVA 2. We make an architecture-wide commitment to predict-then-correct learning. Predict-then-correct can be implemented in MINERVA 2 as *discrepancy encoding* [7, 17]. Given a sequence of observations, MINERVA 2 can predict the next observation in the sequence based on past experience. After the prediction, a new observation is made. We update memory with the *difference* between the observation  $\mathbf{x}$  and the prediction  $\mathbf{e}$ ,  $\mathbf{x} - \mathbf{e}$ , such that if the prediction is correct, no change is made to memory, whereas if the prediction is wrong, that prediction is inhibited in similar contexts in the future.

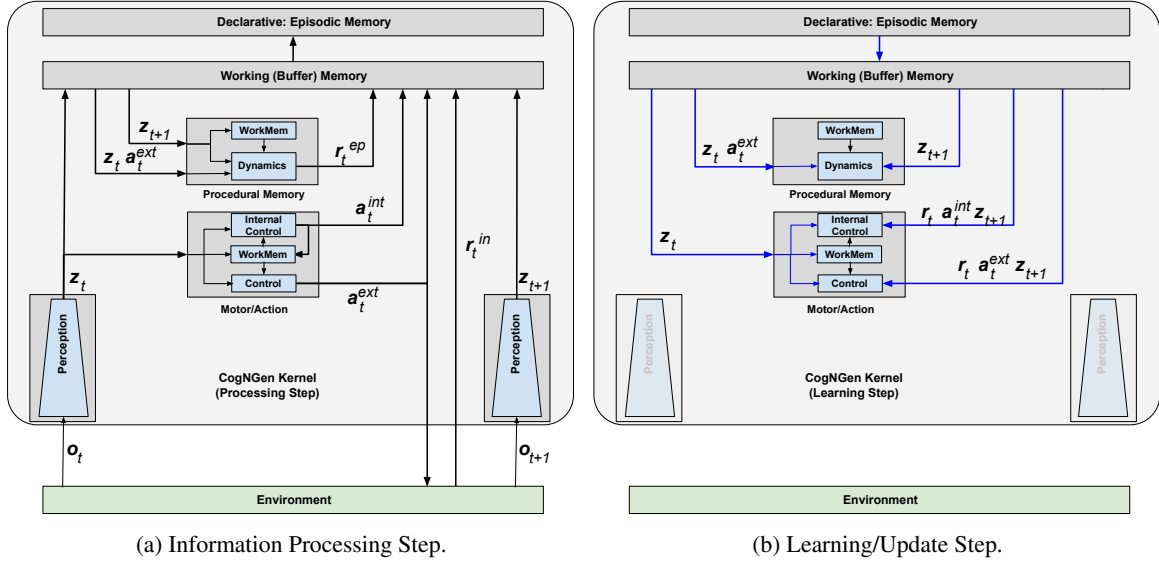


Figure 2: The CogNGen kernel architecture, depicted both in its information processing step/mode (Left) and in its synaptic updating step/mode (Right). Black solid arrows indicate passing of data (which could be one or more vectors of information) while blue solid arrows indicate passing of data (possibly in batches) to facilitate synaptic parameter updating (learning). Notice that the episodic memory is used to instantiate/drive this learning step by forcing it to recollect samples of transition sequences, transferring this to a working buffer which is then used to transfer relevant portions of this recollection to procedural memory module and the motor-action module. Since, in this study, the perception module is a fixed task-provided encoder, no updating is required for this module (and it is thus not active in the learning step of the cognitive kernel).

### 3.3.4 Short-Term vs. Long-Term Memory

Hintzman [16] divides memory into *primary* and *secondary memory*, which loosely correspond to short-term and long-term memory or, in the Common Model of Cognition (Fig. 1), working and declarative memory. The different terminology carry a history of theoretical differences, but signal agreement that there are two kinds of memory: a short-term limited capacity store, and a long-term large capacity store. While Hintzman [16] proposes MINERVA 2 as a theory of *secondary* memory, models of primary and second memory both rely on the same Hebbian learning principles, differing mainly in their capacity limits [25].

For CogNGen, we adopt [7]’s approach and model both working and declarative memory using MINERVA 2. Our working MINERVA 2 is cleared after a task is completed (i.e., a maze is solved), whereas the contents of the declarative MINERVA 2 (which serves as the episodic memory in this paper’s instantiation of CogNGen) persist across tasks.

## 4 The CogNGen Kernel

In this section, we describe the modules that make up the implemented kernel of the CogNGen cognitive architecture, shown in Figure 2.

### 4.1 Perception

CogNGen’s perceptual module transforms or encodes a raw observation pattern vector  $\mathbf{o}_t \in \mathcal{R}^{D_o \times 1}$  at time  $t$  to a latent distributed vector  $\mathbf{z}_t \in \mathcal{R}^{D_z \times 1}$ , where  $D_o$  is the dimensionality of an observation space of some particular modality (visual pixel space, audio waveform space, discrete symbolic token space, etc.) and  $D_z$  is the dimensionality of the latent space. In other words, the perception module should provide an encoding function  $f_e: \mathbf{o}_t \mapsto \mathbf{z}_t$ . If multiple modalities are present, then (at least) one encoder would be allocated per modality. The encoding function provides the benefit of nonlinear mapping of potentially high dimensional sensory spaces to smaller, more manageable ones.

In general, an NGC circuit can be constructed to serve the role of the encoder  $f_e$  for CogNGen. Doing so would yield the additional advantage that a top-down directed generative model, or decoder  $f_g: \mathbf{z}_t \mapsto \mathbf{o}_t$ , would be learned implicitly with  $f_e$ , given that, in prior work, we have shown that NGC learns a good density estimator of data (from which new samples can be “fantasized” or synthesized) [39, 40]. An NGC encoder would, by default, be unsupervised, especially if it is being pre-trained before a task’s simulation, i.e., the NGC  $f_e$  would be trained to predict  $\mathbf{o}_t$  given  $\mathbf{z}_t$ , where  $\mathbf{z}_t$  is iteratively crafted by the NGC settling process described in Section 3.2 (and a feedforward model can be trained to approximate and amortize the settling process to further reduce computational complexity). Having a decoder would also allow for visual interpretation of the distributed representations acquired by CogNGen since a latent vector  $\hat{\mathbf{z}}_t$  (such one produced by the procedural dynamics model, described later) could be run through the underlying top-down directed generative  $f_g$  to produce its corresponding instantiation  $\hat{\mathbf{o}}_t$  in observation space.

Another advantage of the encoder formulation is that if a task-specific (pre-trained/pre-designed) encoder  $f_e$  for a given modality is available, it may be utilized alongside or in place of the NGC encoder model described above. This can simplify and speed up the simulations involving CogNGen, especially if learning a joint perceptual-memory-control system is not the goal, allowing the experimenter to leverage a reliable, stable state representation to design or experiment with various configurations/alterations of the CogNGen kernel’s other internal sub-systems and observe their impact on the task at hand.

In this study, since the environment that we investigate, Gym-Minigrid, provides a fixed, problem-specific encoder  $f_e$  and decoder  $f_g$ , we use a fixed encoding and decoding scheme to simplify our simulations. Future work will build upon the results in this study to investigate learning the perception modules as NGC circuits instead.

## 4.2 Neural Generative Procedural Memory

As demonstrated in neuro-behavioral studies, reward signals are used to evaluate whether or not an action (i.e., motor activity) is desirable or undesirable [41]. Specifically, action selection is driven by changes in the neural activity of the basal ganglia which estimate the value of the expected reward [14]. Motivated by the finding of expected value estimation in the brain, the CogNGen kernel’s procedural module implements a neural circuit that produces intrinsic reward signals. At a high level, this neural machinery facilitates some of the functionality offered by the basal ganglia and procedural memory, simulating an internal reward-creation process [45]. Concretely, we implement an NGC dynamics model from which a reward signal is calculated as a function of its own error neurons. Furthermore, we couple a short-term memory module, based on MINERVA 2, that plays the role of “episodic filtering” (we will also refer to this memory module as a “memory filter”), which is a process that we will develop later in this section which allows the short-term memory to correct/adjust the reward value produced by the dynamics circuit by determining if an observed latent state is familiar or not.

In Figure 3 (Left), we graphically depict the design of the NGC dynamics model used to generate epistemic rewards (or intrinsic reward values meant to encourage exploration). This circuit takes in as input the current latent state  $\mathbf{z}_t$  and the current external action  $\mathbf{a}_t^{ext}$ <sup>1</sup> to be taken by CogNGen (as produced by the motor-action model, see Section 4.3) and predicts the value of the future next step,  $\mathbf{z}_{t+1}$ . In particular, when provided with  $\mathbf{z}_{t+1}$ , the dynamics circuit runs the following equations for its layer-wise predictions:

$$\bar{\mathbf{z}}^2 = \mathbf{W}_{ext}^3 \cdot \mathbf{a}_t^{ext} + \mathbf{W}_z^3 \cdot \mathbf{z}_t + \mathbf{b}_2 \quad (6)$$

$$\bar{\mathbf{z}}^1 = \mathbf{W}^2 \cdot \phi(\bar{\mathbf{z}}^2) + \mathbf{b}_1 \quad (7)$$

$$\hat{\mathbf{z}}_{t+1} = \bar{\mathbf{z}}^0 = g^0(\mathbf{W}^1 \cdot \phi(\bar{\mathbf{z}}^1) + \mathbf{b}_0) \quad (8)$$

and leverages Equation 1 to compute its internal state layer values, i.e.,  $\mathbf{z}_t^3, \bar{\mathbf{z}}_t^2, \bar{\mathbf{z}}_t^1$ . Notice that we have simplified a few items with respect to the NGC circuit – the topmost layer-wise prediction  $\bar{\mathbf{z}}_t^3$  sets  $\phi^3(\mathbf{v}) = \mathbf{v}$  for both its topmost inputs  $\mathbf{a}_t^{ext}$  and  $\mathbf{z}_t$ , the post-activation prediction functions for the internal layers are  $g^2(\mathbf{v}) = g^1(\mathbf{v}) = \mathbf{v}$ , and  $\phi(\mathbf{v}) = \phi^1(\mathbf{v}) = \phi(\mathbf{v})$  (the same state activation function type is used in calculating  $\hat{\mathbf{z}}^1$  and  $\hat{\mathbf{z}}^0$ ). Once the above dynamics have been executed, Equation 2 can be used to adjust the synaptic parameters of the dynamics circuit. Furthermore, upon receiving  $\mathbf{z}_{t+1}$ , the MINERVA 2 episodic memory filter that is coupled to the dynamics circuit stores the latent state vector, updating its current knowledge about the episode that CogNGen is operating with, and outputs a similarity score  $s^{recall}$ . Crucially note that at the end of any particular episode, the contents of the episodic memory filter are cleared/reset upon termination of an episode.

<sup>1</sup>Note that  $\mathbf{a}_t^{ext} \in \{0, 1\}^{A_{ext} \times 1}$  is a one-hot encoding of discrete action  $a_t^{ext}$  and  $A_{ext}$  is the number of different actions possible, as defined by the problem/task.

To generate the value of the epistemic reward [38]), the dynamics model first settles to a prediction  $\hat{\mathbf{z}}_{t+1}$  using the equations above given the value of CogNGen's next latent state  $\mathbf{z}_{t+1}$ . After its settling process has finished, the activity signals of its (squared) error neurons are summed to obtain what is known as the NGC circuit's *total discrepancy* (ToD) [38]. Formally, the epistemic reward signal and final intrinsic reward is computed as follows:

$$r_t^{ep} = \sum_j (\mathbf{e}^0)_{j,1}^2 + \sum_j (\mathbf{e}^1)_{j,1}^2 + \sum_j (\mathbf{e}^2)_{j,1}^2 \quad (9)$$

$$r_t^{ep} = r_t^{ep} / (r_{max}^{ep}) \quad \text{where } r_{max}^{ep} = \max(r_1^{ep}, r_2^{ep}, \dots, r_t^{ep}) \quad (10)$$

where we see the epistemic reward signal is normalized to the range of  $[0, 1]$  by tracking the maximum epistemic signal observed throughout the course of the simulation. This signal is next modified by the short-term memory filter, by modifying the signal as follows:

$$r^{ep} = \begin{cases} \eta_e r^{ep} & s^{recall} \leq s_\theta \\ -0.1 & \text{otherwise} \end{cases} \quad (11)$$

where  $s_\theta$  is an adjustable threshold that  $s^{recall}$  is compared against and  $0 \leq \eta_e \leq 1$  is meant to weight the epistemic signal. In essence, if  $s^{recall} \leq s_\theta$ , then  $\mathbf{z}_{t+1}$  is deemed unfamiliar/surprising and the agent is positively rewarded with the epistemic reward for uncovering a new (latent) state representation of its environment. Whereas if the opposite is true ( $s^{recall} > s_\theta$ ), then the latent state is deemed familiar and the agent is provided with a negative penalty. Finally, the ultimate reward signal is computed by combining the epistemic signal with the problem-specific, instrumental (or extrinsic) reward value  $r_t^{in}$ , i.e.,  $r_t = r_t^{in} + r_t^{ep}$ . Note that, in this study, although we utilize the sparse reward signal provided by the task environment as  $r_t^{in}$ , we remark that another circuit, serving as the system's prior preference model (and thus generator of the instrumental signal itself), could be designed to encode task-specific constraints or probability distributions over preferred goal states [11, 38].

### 4.3 Neural Generative Motor Control

An agent must not merely react to its environment but must also manipulate it. To do so, the agent needs neural circuits to drive its actuators. Building upon the notion of planning-as-inference [3], as in [38], we generalize NGC to the case of action-driven tasks, which we call *active neural generative coding* (ANGC).

Specifically, we design a motor-action model  $f_a: \mathbf{z}_t \mapsto (\mathbf{c}_t^{int}, \mathbf{c}_t^{ext})$  (which offers some of the functionality provided by the motor cortex) that outputs two control signals at each time step, i.e., internal control signal  $\mathbf{c}_t^{int} \in \mathcal{R}^{A_{int} \times 1}$  and external control signal  $\mathbf{c}_t^{ext} \in \mathcal{R}^{A_{ext} \times 1}$ . Note that a discrete internal action  $a_t^{int} \in \{1, 2, \dots, i, \dots, A_{int}\}$  is extracted via  $a_t^{int} = \arg \max_i \mathbf{c}_t^{int}$  and external action  $a_t^{ext} \in \{1, 2, \dots, j, \dots, A_{ext}\}$  is extracted via  $a_t^{ext} = \arg \max_j \mathbf{c}_t^{ext}$  where  $A_{int}$  is the number of discrete internal allowable actions and  $A_{ext}$  is the number of discrete external allowable actions<sup>2</sup>. Action  $a_t^{ext}$  ultimately impacts/affects the environment that the CogNGen system is currently interacting with while action  $a_t^{int}$  affects/manipulates the action model's coupled working memory.

Notably, within the NGC action-motor model is a modifiable working memory that allows the model to store a finite quantity  $M_w$  of projected latent state vectors into a set of self-recurrent memory vectors slots. This particular working memory module, which we call the *self-recurrent slot buffer* (see Figures 1 and 2) serves as the glue that joins the modules of CogNGen together. Working memory in the Common Model of Cognition can be implemented in a variety of ways [33]. In the ACT-R cognitive architecture [1, 2], for example, the mind/brain is understood as consisting of modules connected by buffers. Each buffer is able to maintain information through time and stores data in a small, finite number of slots. Collectively, these buffers serve as ACT-R's working memory. The self recurrent slot buffers in CogNGen serve the same purpose as ACT-R's buffers. Each memory slot in the buffer is represented by  $\mathbf{m}^i \in \mathcal{R}^{M_d \times 1}$  ( $M_d$  is the dimesionality of the memory slot). This component of the action-motor model is inspired by the working memory model proposed in [29]. Concretely, the self-recurrent slot buffer operates according to the following dynamics:

$$\mathbf{k}_t^i = \mathbf{Q}^i \cdot \mathbf{z}_t, \forall i = 1, \dots, M_w \quad // \text{Compute key} \quad (12)$$

$$s^i = \mathbf{s}^i = \frac{1}{|\mathbf{m}^i|} \left( \sum_j [\mathbf{m}^i - \mathbf{k}_t^i]_{j,1} + [\mathbf{k}_t^i - \mathbf{m}^i]_{j,1} \right) \quad // \text{Compute match} \quad (13)$$

$$\mathbf{m}_t = \left[ [\mathbf{m}^1, \mathbf{s}^1], \dots, [\mathbf{m}^i, \mathbf{s}^i], \dots, [\mathbf{m}^{M_w}, \mathbf{s}^{M_w}] \right] \quad // \text{Compute value} \quad (14)$$

<sup>2</sup>In this study, we focus on discrete actions though generalizations to continuous actions are plausible.

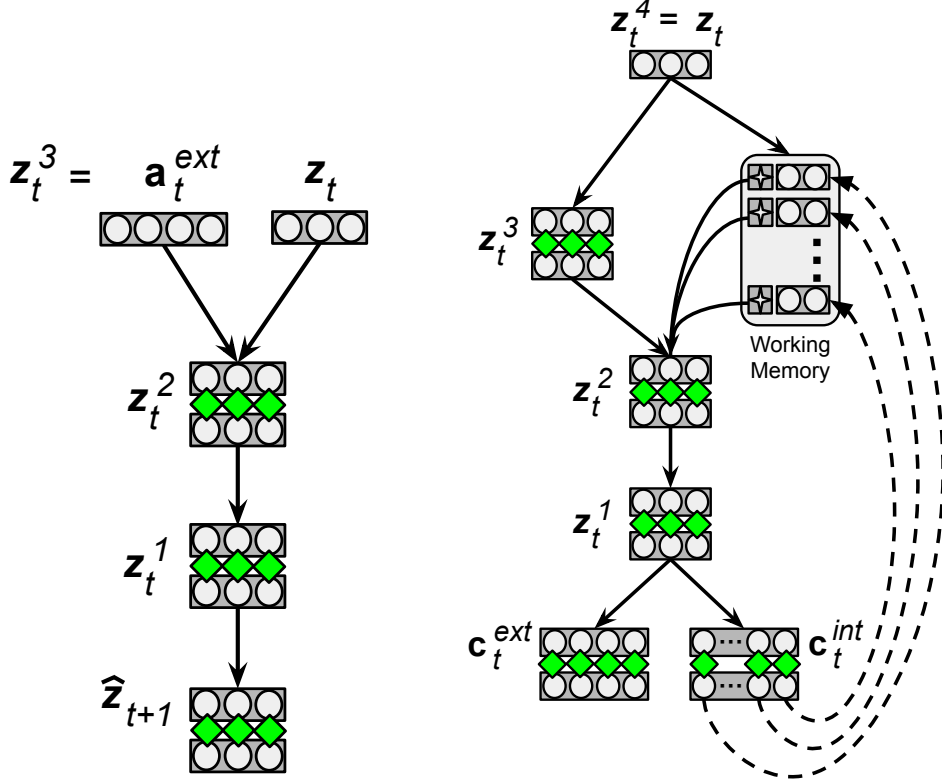


Figure 3: (Left) The CogNGen dynamics model. (Right) The CogNGen kernel motor-action model. Solid arrows represent transformation of data across synaptic weights while dashed arrows represent data passing. Gray circles represent stateful neurons and green diamonds represent error neurons. In the motor model, the internal control portion of the model produces signals  $c_t^{\text{int}}$  that manipulate working memory and the external control portion transmits signals  $c_t^{\text{ext}}$  that affect the environment. Note that internal and control modules are merged together within one circuit and share the same working memory slot module.

where  $\mathbf{Q}^i \in \mathcal{R}^{M_d \times D_z}$  is the  $i$ th random projection matrix (sampled from a centered Gaussian distribution in this paper), which means there is one projection matrix per working memory slot. Note that the match score for any slot  $i$  is  $\mathbf{s}^i = \mathcal{R}^{1 \times 1}$  (a  $1 \times 1$  vector) and thus also a scalar  $s^i$ . The memory module above, in essence, computes a key value vector  $\mathbf{k}_i^i$  given the current state input  $\mathbf{z}_t$  for each slot (by projecting via matrix  $\mathbf{Q}^i$ ), calculates the match score between the  $i$ th key and  $i$ th slot/value, and then returns the entire concatenated contents  $\mathbf{m}_t$  of working memory (including the match scores).

Given the output of working memory  $\mathbf{m}_t$ , the motor-action model then proceeds to compute its output control signal vectors using the ancestral projection scheme described in Section 3.2, yielding  $\mathbf{c}_t^{\text{ext}}, \mathbf{c}_t^{\text{int}} = f_{\text{proj}}(\mathbf{z}_t; \Theta)$ , but with the following modified equations for its layer-wise predictions:

$$\bar{\mathbf{z}}_t^3 = \mathbf{W}^4 \cdot \mathbf{z}_t + \phi(\mathbf{M} \cdot \mathbf{m}_t) + \mathbf{b}^3 \quad (15)$$

$$\bar{\mathbf{z}}_t^2 = \mathbf{W}^3 \cdot \phi(\mathbf{z}_t^3) + \mathbf{b}^2 \quad (16)$$

$$\bar{\mathbf{z}}_t^1 = \mathbf{W}^2 \cdot \phi(\mathbf{z}_t^2) + \mathbf{b}^1 \quad (17)$$

$$\mathbf{c}_t^{\text{ext}} = \bar{\mathbf{z}}_{t,\text{ext}}^0 = \mathbf{W}_{\text{ext}}^1 \cdot \phi(\mathbf{z}_t^1) + \mathbf{b}_{\text{ext}}^0 \quad (18)$$

$$\mathbf{c}_t^{\text{int}} = \bar{\mathbf{z}}_{t,\text{int}}^0 = \mathbf{W}_{\text{int}}^1 \cdot \phi(\mathbf{z}_t^1) + \mathbf{b}_{\text{int}}^0. \quad (19)$$

Note that the above equations are used within not only the ancestral projection scheme described but also in the NGC settling process in tandem with the state update equation, i.e., use Equation 1 to update the internal values of  $\mathbf{z}_t^3, \mathbf{z}_t^2, \mathbf{z}_t^1$ . Note that the synaptic weight matrices are collectively stored in  $\Theta = \{\mathbf{W}_{\text{ext}}^1, \mathbf{b}_{\text{ext}}^0, \mathbf{W}_{\text{int}}^1, \mathbf{b}_{\text{int}}^0, \mathbf{W}^2, \mathbf{b}^1, \mathbf{W}^3, \mathbf{b}^2, \mathbf{W}^4, \mathbf{b}^3, \mathbf{M}\}$ .

The NGC circuit depicted in Equations 15-19 embodies both the ‘internal control’ and ‘control’ sub-systems shown in Figure 2 by outputting  $\bar{\mathbf{z}}_{t,\text{ext}}^0$ , which is the same as control signal vector  $\mathbf{c}_t^{\text{ext}}$ , and  $\bar{\mathbf{z}}_{t,\text{int}}^0$ , which is the

same as control signal vector  $\mathbf{c}_t^{int}$ . The above dynamics represent a five-layer NGC circuit with its top-most layer inputs as  $\mathbf{z}_t^4 = \mathbf{z}_t$  and  $\mathbf{m}_t$ . Furthermore, observe that, for the motor-action model implemented in this paper, we made the following simplifications:  $g^3(\mathbf{v}) = g^2(\mathbf{v}) = g^1(\mathbf{v}) = g^0(\mathbf{v}) = \mathbf{v}$  (all layer-wise prediction post-activation functions set to be the identity) and  $\phi^4(\mathbf{v}) = \phi^3(\mathbf{v}) = \phi^2(\mathbf{v}) = \phi^1(\mathbf{v}) = \phi(\mathbf{v})$  (all state post-activation functions are set to be the same type).

Finally, once the motor-action model has produced its set of control signal vectors, as mentioned at the start of this section, the internal action is selected via  $a_t^{int} = \arg \max_j \mathbf{c}_t^{int}$  and the external action is selected via  $a_t^{ext} = \arg \max_j \mathbf{c}_t^{ext}$ . While  $a_t^{ext}$  is transmitted to the environment<sup>3</sup>,  $a_t^{int}$  is used to modify the working memory module. The internal actions possible are specifically:  $a_t^{int} = \{\text{ignore}, \text{store}_1, \text{store}_2, \dots, \text{store}_{M_w}\}$  (each integer has been mapped to a string clarifying the action's effect), where "ignore" means that the model will ignore  $\mathbf{z}_t$  and not store it into any of the memory slots and "store<sub>i</sub>" means that the model will store  $\mathbf{z}_t$  into memory slot  $i$ .

To update the motor-action model's synaptic efficacies, we then leverage the reward  $r_t$  computed by the dynamics model described in Section 4.2. Specifically, we compute the target control vectors  $\mathbf{z}_{t,ext}^0$  and  $\mathbf{z}_{t,int}^0$  as follows:

$$\mathbf{c}_t^{ext}, \mathbf{c}_t^{int} = f_{proj}(\mathbf{z}_{t+1}; \Theta) \quad (20)$$

$$z_{ext}^0 = \begin{cases} r_t & \text{if } \mathbf{z}_t \text{ is terminal} \\ r_t + \gamma \max_a \mathbf{c}_t^{ext} & \text{otherwise} \end{cases} \quad (21)$$

$$z_{int}^0 = \begin{cases} r_t & \text{if } \mathbf{z}_t \text{ is terminal} \\ r_t + \gamma \max_a \mathbf{c}_t^{int} & \text{otherwise} \end{cases} \quad (22)$$

and the final target vectors computed simply as:

$$\begin{aligned} \mathbf{z}_{t,ext}^0 &= z_{ext}^0 \mathbf{a}_t^{ext} + (1 - \mathbf{a}_t^{ext}) \odot \mathbf{c}_t^{ext} \\ \mathbf{z}_{t,int}^0 &= z_{int}^0 \mathbf{a}_t^{int} + (1 - \mathbf{a}_t^{int}) \odot \mathbf{c}_t^{int}. \end{aligned}$$

Once the target vectors have been created, the NGC settling process can be executed and all synaptic parameters  $\Theta$  of the motor-action model are updated using Equation 2.

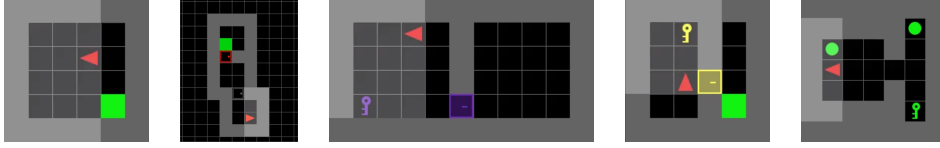
#### 4.4 Explicit Declarative Memory: Episodic Memory

In the context of reinforcement learning, in order to crucially improve the stability and convergence of artificial neural networks trained over many episodes, each containing often many transitions, experience replay is typically used [36]. In early studies of rats, neural replay sequences were detected in the hippocampus [46] during rest, where "place" cells spontaneously and rapidly fired in such a way as to represent the previous paths traversed by the animals while awake. These "replay" sequences would only last nearly a fraction of a second but covered several seconds of real-world experience. Similar replay effects have been recently been studied/detected in human subjects [30], providing further biological justification of the replay buffer used in modern-day RL neural systems.

CogNGen also implements a replay mechanism in the form an episodic memory constructed with MINERVA. Information is transferred to this memory through an intermediate working buffer, where pieces of a transition (partial experience) are progressively stored as they are encountered throughout the agent-environment interaction process. Specifically, once the buffer contains at least a partial transition  $(\mathbf{z}_t, \mathbf{a}_t^{ext}, \mathbf{a}_t^{int}, \mathbf{r}_t)$  where  $\mathbf{r}_t \in \mathcal{R}^{1 \times 1}$  (ensuring the reward scalar is in vector form), our episodic memory module  $\mathcal{M}$  (which is created alongside a starting transition buffer  $\mathcal{S}_0$ ) is updated iteratively according to the following algorithm:

1. Create a window (buffer)  $w$  of length  $L$  – each slot is filled with empty values (zero vectors of the correct length). Store the start transition  $\mathbf{m}_0^{exp} = [\mathbf{z}_0, \mathbf{a}_0^{ext}, \mathbf{a}_0^{int}, \mathbf{r}_0]$  in buffer  $\mathcal{S}_0$ .
2. Store  $\mathbf{m}_t^{exp} = [\mathbf{z}_t, \mathbf{a}_t^{ext}, \mathbf{a}_t^{int}, \mathbf{r}_t]$  at the last position (index  $L$ ) of the window  $w$  and delete the entry at position 0.
3. Flatten  $w$  into a single vector  $\mathbf{w}_{mem}$  and store this item by updating episodic memory  $\mathcal{M}$ .
4. If episode terminal has been reached, go to Step 1, else go to Step 2.

<sup>3</sup>Alternatively, this action is a high-level signal that would be fed into another sub-system, such as a nervous system model that is responsible for translating the  $a_t^{ext}$  to lower-level commands to move a limb or control another actuator system.



	Average Success Rate				R6x6	Average Episode Length			
	MR	Unl	DK	Mem		MR	Unl	DK	Mem
DQN	99.50	0.00	0.00	0.00	40.0	9.31	100.0	100.0	100.0
RnD	100.00	90.00	100.0	100.0	48.5	3.50	31.46	4.08	3.71
BeBold DQN-CNT	100.00	98.00	100.0	100.0	48.0	3.98	23.51	4.46	3.93
CogNGen	100.00	98.50	100.0	100.0	98.5	3.90	23.41	4.15	5.48

Table 1: In the top row, examples of the four tasks we experimented with in this paper are presented graphically – from left to right, the random  $6 \times 6$  empty room task (R6  $\times$  6), the multi-room task with three rooms and each of size four (MR), the unlock task (Unl), the door-key task (DK), and the memory task (Mem). In the bottom row, we present results for the: (Left) Average success rate (%) over the last 100 episodes. (Right) Average episode length (% of maximum/worst-case episode length - closer to 0 is better/more efficient) over the last 100 episodes.

The above algorithmic memory updating process is repeated continually until the end of the simulation. Note that we also impose an upper bound on the total number of transitions stored in  $\mathcal{M}$  (as is done with standard experience replay buffer implementations) – if this upper bound is exceeded, we remove the earliest transition stored  $\mathbf{m}_t^{exp}$  in  $\mathcal{M}$  and update  $\mathcal{S}_0$  accordingly.

To sample an episode from the episodic memory module  $\mathcal{M}$ , the following algorithm is executed:

1. Create window  $w$  of length  $L$ , initialized with empty values. Sample  $\mathbf{m}_0^{exp} \sim \mathcal{S}$ , and place it in the last position  $L$  in  $w$ .
2. Remove the item at position 1 in  $w$  and use  $\mathcal{M}$  to hetero-associatively complete/predict  $\mathbf{m}_{t+1}^{exp}$  via Equation 5.
3. Store  $\mathbf{m}_{t+1}^{exp}$  at last position  $L$  within  $w$ .
4. Repeat steps 2 through 4 until episode terminal reached.

The algorithm above is repeated until  $K$  episodes have been sampled. To create a mini-batch of transitions that can be used to then trigger a synaptic weight update of the motor-action and dynamics models, we randomly sample select/create  $B$  transitions  $(\mathbf{z}_j, \mathbf{a}_j^{ext}, \mathbf{a}_j^{int}, \mathbf{r}_t, \mathbf{z}_{j+1})$  from each sampled episode.

When using the episodic memory  $\mathcal{M}$  above, we do not update the motor-action and dynamics models online but instead update their parameters only when  $\mathcal{M}$  is sampled. This breaks down the CogNGen computational process into two steps/phases at each time step of simulation: 1) the processing step (Figure 2a), followed by 2) the learning step (Figure 2b).

## 5 Experimental Results

In this section, we describe our experimental/simulation setup as well as the CogNGen agent and the baselines evaluated.

### 5.1 The Mini GridWorld Problem

To evaluate CogNGen, we adapt a simulated environment from the OpenAI Gym extension, Mini-GridWorld [5]. Specifically, we investigate two problems/tasks within its collection to evaluate the agents constructed using CogNGen, namely the *Door-Key* task and the *Memory* task. The format of each task’s observation space (which is fundamentally an  $N \times M$  tile grid) is a partially observable view of the agent’s environment, which is created via a compact, efficient encoding of the original pixel space to a  $7 \times 7 \times 3$  tensor (a 3-channel object that is created by mapping each visible grid cell to 3 integer values). Each tile contains either nothing (represented as zero) or one object (which has an associated discrete color and a discrete object type). Ultimately, each tile is encoded to an object index (first channel – 0 means unseen, 1 means empty, 2 means wall, etc.), a color index (second channel – 0 means red, 1 means green, etc.), and a state index (third channel – 0 means open, 1 means closed, 2 means locked).

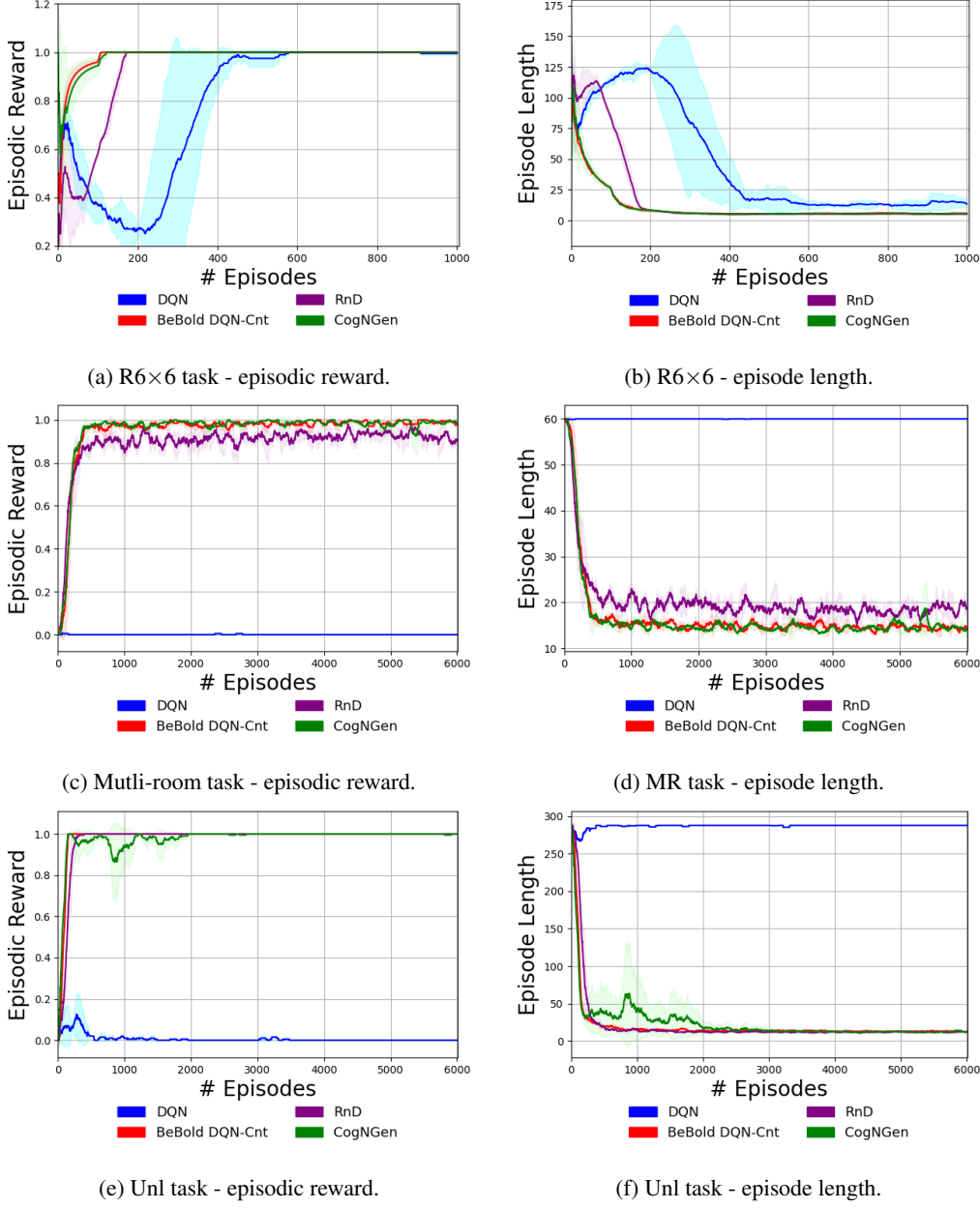


Figure 4: (Left) Average reward and (Right) average episode length (values are smoothed with an averaging window of 100) for (top-to-bottom): random  $6 \times 6$  empty room (R6×6), the multi-room (MR), and the Unlock (Unl) task. Curves depict the mean (solid colored line) and standard deviation (light colored envelope) over five experimental trials.

The agent itself is restricted to picking up one single object, such as a key, and may open a locked door if it carries a key that matches the door’s color. The discrete action space for our agent can be summarized as a set of six unique actions: 1) turn left, 2) turn right, 3) move forward, 4) pick up an object, 5) drop the object that the agent is currently carrying, and 6) toggle/activate (such as opening a door or interacting with an object).<sup>4</sup> The reward structure/signal provided by all problems in the Mini-GridWorld environment is sparse – the agent is only given a positive 1.0 extrinsic reward if it reaches the green goal tile and 0 otherwise, making all problems quite difficult from a reinforcement learning perspective. Each problem has a specific time step limit allotted to allow the agent to complete the task (and maximum episode lengths ranged from 60 to 360 time steps).

<sup>4</sup>Note that we omitted the seventh optional action of raising a “done” signal.

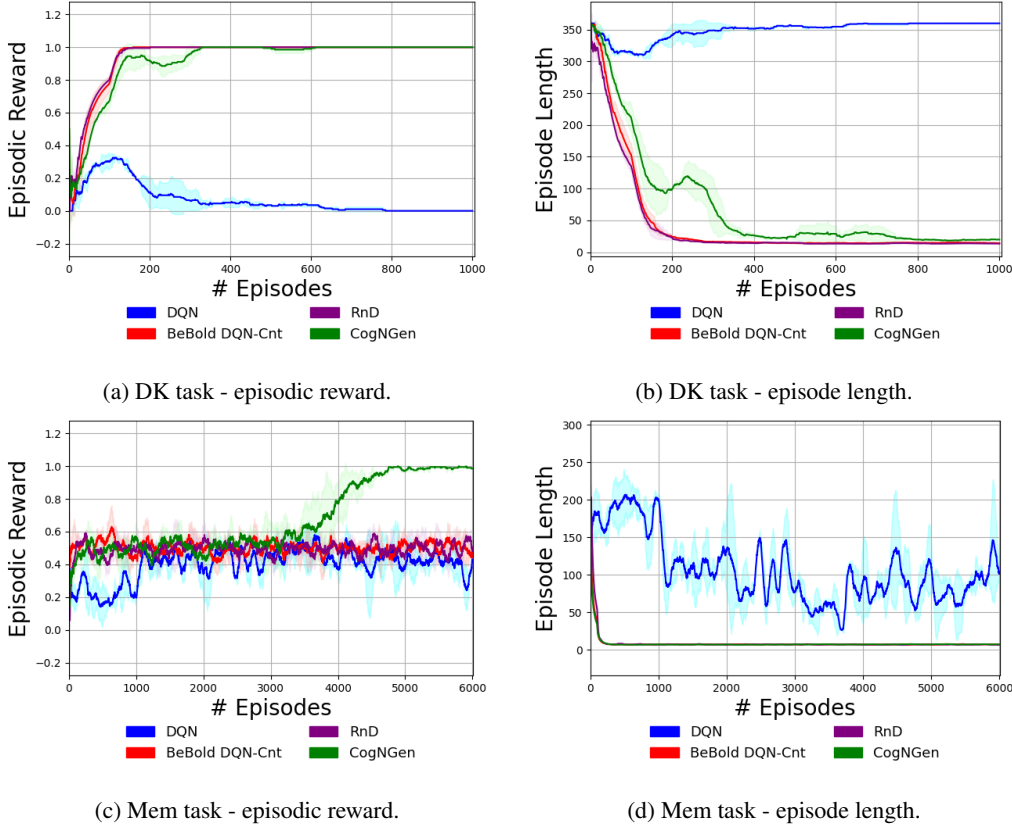


Figure 5: (Left) Average reward and (Right) episode length (values are smoothed with an averaging window of 100) for (top-to-bottom): the door-key (DK) and memory (Mem) task (Right). Curves depict the mean (solid colored line) and standard deviation (light colored envelope) over five experimental trials.

**The Random Empty Room Task:** In this task, the simplest of the ones we investigated, the agent is spawned at a random location (and different starting orientation) within the room and must reach the green goal square, where a sparse reward is provided if the goal is reached before the episode time-out.

**The Multi-Room Task:** This task requires the agent to navigate a series of connected rooms where the agent must open the door in one room in order to proceed to the next room. In the final room, there is a green goal square that the agent must reach in order to terminate the episode successfully. Note that this is a procedurally generated environment and the floor plan is different each episode. We focused on three rooms of size  $4 \times 4$  in this study.

**The Unlocking Task:** In this task, the agent has to open a locked door (in order to successfully exit an episode) by first finding the key that may unlock. The key location, the door position, and the agent initial position/orientation are randomly generated each episode.

**The Door-Key Task:** In this problem, the agent must find a key (the position of which is randomly spawned across episodes) inside a locked room and then pick up the key in order to unlock the door so that it may leave the first room and enter the second one. Upon entering the next room, the agent must find the green tile in order to successfully exit (and terminate the episode by reaching the goal state to receive a positive reward). For this study, we focus on the  $6 \times 6$  room variant of the problem (which offered sufficient complexity to test the agents against).

**The Memory Task:** This problem is posed as a memory test. The agent starts in a small room where it sees an object (such as a key or a ball) – note that we slightly modified the problem to ensure the agent starts the episode looking in the direction of the object. After perceiving the object, the agent must then turn around, exit the room and go through a narrow hallow that ends in a split. At the end of this split, the agent can either go up

or go down, and at the end of each of these splits is a different object (either a key or a ball). To successfully complete the episode (and receive a positive reward), the agent must remember the initial object that it saw and go to the split that contains the correct matching object. For this study, we focus on the size 7 problem ( $7 \times 7$  room variant).

## 5.2 CogNGen Model Instantiation

With respect to the hyper-parameters of the CogNGen kernel agent investigated (referred to as “CogNGen” in all plots/tables), all of the NGC circuits (for both motor-action and dynamics models) were allowed to relax/settle to latent state activities (given clamped input and output sensory values) for  $K = 10$  steps with  $\tau = 10$  (ms). The linear rectifier was used as the state activation function  $\phi(\mathbf{v})$  for all neural circuits. All NGC synapses were initialized from a centered Gaussian distribution with standard deviation  $\sigma = 0.05$ . The values within an environment encoding vector  $\mathbf{z}_t$  (produced by the fixed encoder) were further normalized such that each was in the range of  $[0, 1]$ ).

The motor-action model contained two latent state layers of 512 neurons and the number of input sensory neurons was set equal to the environment encoding space, i.e., 147 elements, while the number of external control neurons was set equal to the number of discrete actions, i.e., 6, and the number of internal control neurons set to  $K + 1$  (where  $K$  was the number of working memory slots used for the action model’s coupled working memory, typically set in the range of 1 – 3). The dynamics model also contained two latent state layers, but each contained 128 neurons, and its coupled episodic memory filter was allowed to store as many memory vectors needed to equal to the length of the current episode (which were often of variable length). The large episodic declarative memory module was allowed to store up to 100,000 memory vectors (window  $w$  length was  $L = 20$ ) and was configured to use a memory power coefficient  $p = 100$  and a very small forgetting rate of 0.0001. (and the additional constraint was imposed to ensure that the total number of memory vectors never exceeded 100,000 whenever a vector was stored, meaning that the earliest vector in  $\mathcal{M}$  had to be deleted and  $S_0$  adjusted accordingly).

All NGC circuit synaptic efficacies were adjusted by computing their updates as described in the earlier in Section 4.4 (the learning step of CogNGen) and using the Adam adaptive learning rate [27], with a step size  $\eta = 0.0005$ , to ultimately apply the synaptic parameter adjustments. An epsilon-greedy policy was used in early episodes of CogNGen’s external action selection, where an  $\epsilon_{ext} = 0.95$  was used for the external actions and  $\epsilon_{int} = 0.1$  was used for the internal actions with both  $\epsilon_{ext}$  and  $\epsilon_{int}$  exponentially decayed to 0.0.

## 5.3 Baseline Models

We compare the CogNGen to several baseline models: a standard deep Q-network (DQN) [36], a DQN that leverages an intrinsic reward generated through random network distillation (RnD) [4] (a powerful intrinsic curiosity model), and a DQN that learns through a count-based formulation of the BeBold exploration framework [51] (BeBold DQN-CNT). The DQN component of each of the above baselines utilized two layers of hidden neurons (the size of which were searched in the range of 128 through 512) using the linear rectifier activation function. For RnD, the predictor  $\hat{f}(\mathbf{z}_{t+1})$  and random target network  $f(\mathbf{z}_{t+1})$  both contained two layers neurons (size of which was searched in range of 128 through 512) also using the linear rectifier activation. The weight parameters for all DQNs as well as the RnD’s predictor and random networks were initialized according to the scheme of [12] and parameters were optimized by calculating gradients using reverse-mode differentiation and the Adam adaptive learning rate with step size searched in the range 0.0002 through 0.001. The BeBold DQN-CNT utilized global state visitation counts to compute its intrinsic reward bonus (meaning that we implemented and tuned the “episodic restriction on intrinsic reward”, or ERIR, model in [51]). Specifically, our implementation of the intrinsic reward for the BeBold model was calculated specifically as follows:

$$r^i = \max \left( 0, \frac{1}{\mathbb{N}(\mathbf{z}_{t+1})} - \frac{1}{\mathbb{N}(\mathbf{z}_t)} \right) \left( \mathbb{1} \left\{ \frac{1}{\mathbb{N}_e(\mathbf{z}_{t+1})} \right\} \right)$$

$$r_t^i = (r^i > 0 \rightarrow r^i) \wedge (r^i \leq 0 \rightarrow -\alpha)$$

where  $0.1 \leq \alpha \leq 1$  and  $\mathbb{N}(\mathbf{z}_t)$  is the hash table that returns the global visitation of state  $\mathbf{z}_t$  while  $\mathbb{N}_e(\mathbf{z}_t)$  returns the episodic visitation count of  $\mathbf{z}_t$ . Note that the key needed to retrieve is the count value is the  $x$ - $y$  coordinate of state  $\mathbf{z}_t$  extracted from the problem environment. For RnD, our implementation of the intrinsic reward proceeded

as follows:

$$r^i = \left( \|\hat{f}(\mathbf{z}_{t+1}) - f(\mathbf{z}_{t+1})\|_2^2 \right) \left( \mathbb{1} \left\{ \frac{1}{\mathbb{N}_e(\mathbf{z}_{t+1})} \right\} \right)$$

$$r_t^i = (r^i > 0 \rightarrow r^i) \wedge (r^i \leq 0 \rightarrow -\alpha)$$

Notice that, in order to obtain robust and stable performance, we had to modify the RnD and BeBold intrinsic bonus calculations in order to learn in the above tasks by imposing a small negative penalty on discrete states that were visited more than once within an episode (meaning that a hash table had to be used to track the global state coordinates and visitation counts of each prior state seen, which was reset at the end of each episode). Note that RnD and BeBold have access to problem-specific, global information from the Mini GridWorld task environments whereas CogNGen and the DQN do not.

#### 5.4 Results and Discussion

In Table 1, we report the average success rate (at solving the task/reaching the goal state) as well as the average episode length (average measurements were computed over the last 100 episodes of training/simulation for all models). In Figures 4 and 5, we present the reward curves (computed as the mean and standard deviation across five simulation runs/experimental trials).

Based on the results of our simulations, we find that (1) CogNGen is able to learn the grid-world tasks, (2) the performance is comparable to / on par with powerful deep intrinsic curiosity RL methods that have access to problem-specific, global information, and (3) that CogNGen can successfully solve and outperform all baselines on the memory task. Given that CogNGen approximates much of the functionality of modern-day RL tricks and mechanisms with large auto-associative Hebbian memory modules and predictive processing circuits, the results uncovered are promising. When comparing the baselines to CogNGen, we notice that there are some instances where the powerful BeBold DQN-CNT and RnD baselines yield shorter episodes or yield higher episodic rewards earlier (after converging to an optimal policy). We reason that this small gap/difference is likely due to: 1) BeBold DQN/RnD have access to global, problem-specific information (the agent’s  $x$ - $y$  coordinates in the world in order to calculate state visitation counts) whereas CogNGen only operates with local information/observations, 2) CogNGen’s mechanism to update synapses relies on an episodic memory system that is imperfect (which is arguably more human-like yet introduces error in the recollections as compared to a standard experience replay buffer), and 3) CogNGen’s motor-action model must also learn how to manipulate its coupled working memory (via internal actions) in addition to how to interact with its environment (via external actions), which requires learning a more complex policy.

## 6 Conclusions and Future Research

In this work, we presented CogNGen (the COGnitive Neural GENerative system), a novel cognitive architecture, or rather, its “kernel” (or core) composed of circuits based on neural generative coding (i.e., predictive processing) and auto-associative Hebbian memory (MINERVA 2). CogNGen lays down the groundwork for designing intelligent agents, composed of neurobiologically-plausible building blocks, that learn across diverse tasks as well as potentially model human performance at larger scales. Our results, on a challenging set of sparse reward reinforcement learning problems, show that the synergy between a classic model of human memory and predictive processing neural circuits can yield viable adaptive systems that elicit goal-directed behavior.

## References

- [1] Anderson, J.R., Lebiere, C.: The atomic components of thought. Lawrence Erlbaum Associates, Mahwah, NJ (1998)
- [2] Anderson, J.R.: How can the human mind occur in the physical universe? Oxford University Press, New York, NY (2009)
- [3] Botvinick, M., Toussaint, M.: Planning as inference. *Trends in Cognitive Sciences* **16**(10), 485–488 (2012)
- [4] Burda, Y., Edwards, H., Storkey, A., Klimov, O.: Exploration by random network distillation. arXiv preprint arXiv:1810.12894 (2018)
- [5] Chevalier-Boisvert, M., Willems, L., Pal, S.: Minimalistic gridworld environment for openai gym. <https://github.com/maximecb/gym-minigrid> (2018)

[6] Clark, A.: *Surfing uncertainty: Prediction, action, and the embodied mind*. Oxford University Press (2015)

[7] Collins, R.N., Milliken, B., Jamieson, R.K.: MINERVA-DE: An instance model of the deficient processing theory. *Journal of Memory and Language* **115**, 104151 (2020). <https://doi.org/10.1016/j.jml.2020.104151>

[8] Dougherty, M.R.P., Gettys, C.F., Ogden, E.E.: MINERVA-DM: A memory processes model for judgments of likelihood. *Psychological Review* **106**, 180–209 (1999). <https://doi.org/10.1037/0033-295X.106.1.180>

[9] French, R.M.: Catastrophic forgetting in connectionist networks. *Trends in Cognitive Sciences* **3**(4), 128–135 (1999)

[10] Friston, K.: A theory of cortical responses. *Philosophical transactions of the Royal Society B: Biological sciences* **360**(1456), 815–836 (2005)

[11] Friston, K., FitzGerald, T., Rigoli, F., Schwartenbeck, P., Pezzulo, G.: Active inference: a process theory. *Neural computation* **29**(1), 1–49 (2017)

[12] He, K., Zhang, X., Ren, S., Sun, J.: Delving deep into rectifiers: Surpassing human-level performance on imagenet classification. In: *Proceedings of the IEEE international conference on computer vision*. pp. 1026–1034 (2015)

[13] Hebb, D.O.: The organization of behavior: A neuropsychological theory (1949)

[14] Hikosaka, O., Nakamura, K., Nakahara, H.: Basal ganglia orient eyes to reward. *Journal of Neurophysiology* **95**(2), 567–584 (2006)

[15] Hintzman, D.L.: Minerva 2: A simulation model of human memory. *Behavior Research Methods, Instruments, and Computers* **16**, 96–101 (1984). <https://doi.org/10.3758/BF03202365>

[16] Hintzman, D.L.: “Schema abstraction” in multiple-trace memory models. *Psychological Review* **93**, 411–428 (1986). <https://doi.org/10.1037/0033-295X.95.4.528>

[17] Jamieson, R.K., Crump, M.J.C., Hannah, S.D.: An instance theory of associative learning. *Learning & Behavior* **40**, 61–82 (2012). <https://doi.org/10.3758/s13420-011-0046-2>

[18] Jamieson, R.K., Mewhort, D.J.K.: Applying an exemplar model to the artificial-grammar task: Inferring grammaticality from similarity. *Quarterly Journal of Experimental Psychology* **62**, 550–575 (2009). <https://doi.org/10.1080/17470210802055749>

[19] Jamieson, R.K., Mewhort, D.J.K.: Grammaticality is inferred from global similarity: A reply to kinder (2010). *The Quarterly Journal of Experimental Psychology* **64**, 209–216 (2011). <https://doi.org/10.1080/17470218.2010.537932>

[20] Jamieson, R.K., Avery, J.E., Johns, B.T., Jones, M.N.: An instance theory of semantic memory. *Computational Brain & Behavior* **1**(2), 119–136 (Jun 2018). <https://doi.org/10.1007/s42113-018-0008-2>, <https://doi.org/10.1007/s42113-018-0008-2>

[21] Johns, B.T., Jamieson, R.K., Crump, M.J.C., Jones, M.N., Mewhort, D.J.K.: The combinatorial power of experience. In: Papafragou, A., Grodner, D., Mirman, D., Trueswell, J.C. (eds.) *Proceedings of the 38th Annual Meeting of the Cognitive Science Society*. pp. 1325–1330. Cognitive Science Society, Austin, TX (2016)

[22] Johns, B.T., Jamieson, R.K., Crump, M.J.C., Jones, M.N., Mewhort, D.J.K.: The combinatorial power of experience. In: Papafragou, A., Grodner, D., Mirman, D., Trueswell, J.C. (eds.) *Proceedings of the 38th Annual Meeting of the Cognitive Science Society*. pp. 1325–1330. Cognitive Science Society, Austin, TX (2016), <https://mindmodeling.org/cogsci2016/papers/0236/>

[23] Kelly, M.A., Arora, N., West, R.L., Reitter, D.: Holographic declarative memory: Distributional semantics as the architecture of memory. *Cognitive Science* **44**(11), e12904 (2020). <https://doi.org/10.1111/cogs.12904>

[24] Kelly, M.A., Ghafurian, M., West, R.L., Reitter, D.: Indirect associations in learning semantic and syntactic lexical relationships. *Journal of Memory and Language* **115**, 104153 (2020). <https://doi.org/10.1016/j.jml.2020.104153>

[25] Kelly, M.A., Mewhort, D.J.K., West, R.L.: The memory tesseract: Mathematical equivalence between composite and separate storage memory models. *Journal of Mathematical Psychology* **77**, 142–155 (2017). <https://doi.org/10.1016/j.jmp.2016.10.006>

[26] Kersten, L., West, R.L., Brook, A.: Leveling the field: Talking levels in cognitive science. In: Papafragou, A., Grodner, D., Mirman, D., Trueswell, J.C. (eds.) *Proceedings of the 38th Annual Meeting of the Cognitive Science Society*. pp. 2399–2404. Cognitive Science Society, Austin, TX (2016), <https://cogsci.mindmodeling.org/2016/papers/0415/paper0415.pdf>

[27] Kingma, D.P., Ba, J.: Adam: A method for stochastic optimization. arXiv preprint arXiv:1412.6980 (2014)

[28] Kotseruba, I., Tsotsos, J.K.: 40 years of cognitive architectures: Core cognitive abilities and practical applications. *Artificial Intelligence Review* (Jul 2018). <https://doi.org/10.1007/s10462-018-9646-y>

[29] Kruijne, W., Bohte, S.M., Roelfsema, P.R., Olivers, C.N.: Flexible working memory through selective gating and attentional tagging. *Neural Computation* **33**(1), 1–40 (2021)

[30] Kurth-Nelson, Z., Economides, M., Dolan, R.J., Dayan, P.: Fast sequences of non-spatial state representations in humans. *Neuron* **91**(1), 194–204 (2016)

[31] Kwantes, P.J.: Using context to build semantics. *Psychonomic Bulletin & Review* **12**, 703–710 (2005). <https://doi.org/10.3758/BF03196761>

[32] Laird, J.E.: The Soar Cognitive Architecture. MIT Press, Cambridge, MA (2012)

[33] Laird, J.E., Lebiere, C., Rosenbloom, P.S.: A standard model of the mind: Toward a common computational framework across artificial intelligence, cognitive science, neuroscience, and robotics. *AI Magazine* **38**(4), 13–26 (2017). <https://doi.org/10.1609/aimag.v38i4.2744>

[34] Mannering, W.M., Jones, M.N.: Catastrophic interference in predictive neural network models of distributional semantics. *Computational Brain & Behavior* **4**(1), 18–33 (2021)

[35] McCloskey, M., Cohen, N.J.: Catastrophic interference in connectionist networks: The sequential learning problem. *Psychology of Learning and Motivation* **24**(109), 92 (1989)

[36] Mnih, V., Kavukcuoglu, K., Silver, D., Rusu, A.A., Veness, J., Bellemare, M.G., Graves, A., Riedmiller, M., Fidjeland, A.K., Ostrovski, G., et al.: Human-level control through deep reinforcement learning. *Nature* **518**(7540), 529–533 (2015). <https://doi.org/10.1038/nature14236>

[37] Newell, A.: You can't play 20 questions with nature and win. In: Chase, W.G. (ed.) *Visual information processing*, pp. 283–308. Academic Press, New York (1973)

[38] Ororbia, A., Mali, A.: Backprop-free reinforcement learning with active neural generative coding. arXiv preprint arXiv:2107.07046 (2021)

[39] Ororbia, A.G., Kifer, D.: The neural coding framework for learning generative models. arXiv preprint arXiv:2012.03405 (2020)

[40] Ororbia, A.G., Mali, A., Giles, C.L., Kifer, D.: Continual learning of recurrent neural networks by locally aligning distributed representations. *IEEE Transactions on Neural Networks and Learning Systems* (2020)

[41] Rangel, A., Camerer, C., Montague, P.R.: A framework for studying the neurobiology of value-based decision making. *Nature reviews neuroscience* **9**(7), 545–556 (2008)

[42] Rao, R.P., Ballard, D.H.: Predictive coding in the visual cortex: a functional interpretation of some extra-classical receptive-field effects. *Nature Neuroscience* **2**(1) (1999)

[43] Ritter, F.E., Tehranchi, F., Oury, J.D.: Act-r: A cognitive architecture for modeling cognition. *Wiley Interdisciplinary Reviews: Cognitive Science* **10**(3), e1488 (2019). <https://doi.org/10.1002/wcs.1488>

[44] Rosenbloom, P.S., Demski, A., Ustun, V.: The Sigma cognitive architecture and system: Towards functionally elegant grand unification. *Journal of Artificial General Intelligence* **7**(1), 1–103 (2016). <https://doi.org/10.1515/jagi-2016-0001>

[45] Schultz, W.: Reward functions of the basal ganglia. *Journal of neural transmission* **123**(7), 679–693 (2016)

[46] Skaggs, W.E., McNaughton, B.L.: Replay of neuronal firing sequences in rat hippocampus during sleep following spatial experience. *Science* **271**(5257), 1870–1873 (1996)

[47] Steine-Hanson, Z., Koh, N., Stocco, A.: Refining the common model of cognition through large neuroscience data. *Procedia Computer Science* **145**, 813–820 (12 2018). <https://doi.org/10.1016/j.procs.2018.11.026>, papers on the Common Model of Cognition

[48] Stocco, A., Laird, J., Lebiere, C., Rosenbloom, P.: Empirical evidence from neuroimaging data for a standard model of the mind. In: Rogers, T.T., Rau, M., Zhu, X., Kalish, C.W. (eds.) *Proceedings of the 40th Annual Conference of the Cognitive Science Society*. pp. 1094–1099. Cognitive Science Society, Austin, TX (2018), <https://mindmodeling.org/cogsci2018/papers/0216/>

[49] Stocco, A., Sibert, C., Steine-Hanson, Z., Koh, N., Laird, J.E., Lebiere, C.J., Rosenbloom, P.: Analysis of the human connectome data supports the notion of a “common model of cognition” for human and human-like intelligence across domains. *NeuroImage* **235**, 118035 (2021). <https://doi.org/10.1016/j.neuroimage.2021.118035>

- [50] Thomas, R.P., Dougherty, M.R., Sprenger, A.M., Harbison, J.I.: Diagnostic hypothesis generation and human judgment. *Psychological Review* **115**, 155–185 (2008). <https://doi.org/10.1037/0033-295X.115.1.155>
- [51] Zhang, T., Xu, H., Wang, X., Wu, Y., Keutzer, K., Gonzalez, J.E., Tian, Y.: Bebold: Exploration beyond the boundary of explored regions. arXiv preprint arXiv:2012.08621 (2020)